HHS Public Access

Author manuscript

Ann Otol Rhinol Laryngol. Author manuscript; available in PMC 2016 November 01.

Published in final edited form as:

Ann Otol Rhinol Laryngol. 2015 November ; 124(11): 903–910. doi:10.1177/0003489415591205.

Short-Term Peripheral Auditory Effects of Cranial Irradiation: A Mouse Model

Krysta L. Gasser Rutledge, BA, **Kumar G. Prasad, MD**, **Kara R. Emery**, **Anthony A. Mikulec, MD**, **Mark Varvares, MD**, and **Michael Anne Gratton, PhD**

Department of Otolaryngology Head-Neck Surgery, Saint Louis University, St. Louis, MO, USA

Abstract

1. short-term threshold shift
2. short-term peripheral auditory histopathology
3. the mouse as an experimental model

Methods—Adult mice were exposed to single-dose radiation of 10 – 60 Gy. Pre- and post-irradiation (baseline, 2 – 8 days) audiometric brainstem response data were recorded with analysis of cochlear ultrastructure.

Results—Significant threshold shift occurred at all test frequencies in mice exposed to ≥ 20 Gy at 4 – 6 days post-irradiation. Ultrastructurally in Rosenthal's canal and the spiral lamina, neuronal density and extracellular matrix decreased dramatically. There was overall preservation of hair cells, stria vascularis, and vasculature. No difference within Gy group was noted in the frequency or severity of pathology along the length of the cochlea.

Conclusions—The initial impact of radiation in the first week post-exposure focuses on spiral ganglion cell bodies and peripheral projections, resulting in significant threshold shift for irradiation dosages ≥ 20 Gy. This study demonstrates that the mouse is a viable model for study of short-term peripheral auditory effects using single-dose cranial irradiation. Additionally, with access to a precise animal irradiator, the mouse may be used as an experimental model for a fractionated irradiation dosage of 10 Gy, simulating stereotactic therapeutic cranial irradiation.

Keywords

Cranial Irradiation; Short-Term Radiation Effects; Mouse Model; Cochlea; Hearing Loss; Auditory Brainstem Response

---

Reprint Request Contact and Corresponding Author: Michael Anne Gratton, PhD, Department of Otolaryngology Head-Neck Surgery, Saint Louis University Hospital, 3635 Vista Ave. FDT, St. Louis, MO 63110, Telephone: (314) 977 – 5200, Fax: (314) 268 – 5111, mgratton@slu.edu.

Krysta L. Gasser Rutledge, BA: Collected and analyzed data, conducted statistics, wrote manuscript
Kumar G. Prasad, MD: Designed study, collected and analyzed data, revised manuscript
Kara R. Emery: Collected and analyzed data, prepared images, revised manuscript
Anthony A. Mikulec, MD: Study conception, revised manuscript
Mark Varvares, MD: Study conception, revised manuscript
Michael Anne Gratton, PhD: Designed study, analyzed data, conducted statistics, wrote manuscript

This study was performed in accordance with the PHS Policy on Humane Care and Use of Laboratory Animals, the NIH *Guide for the Care and Use of Laboratory Animals*, and the Animal Welfare Act (7 U.S.C. et seq.); the animal use protocol was approved by the Institutional Animal Care and Use Committee (IACUC) of Saint Louis University School of Medicine.

Introduction

Cranial irradiation is a common component of treatment for head and neck malignancies. Various treatment options include fractionated radiation therapy, stereotactic radiosurgery, and fractionated stereotactic radiation therapy (Bhandare et al., 2010). Fractionated vs single doses of cranial irradiation are more commonly used to treat head and neck malignancies because of increased dosage capability to the tumor and lower toxicity for surrounding structures, thus improving post-treatment functionality. However, single or hypofractionated dosage stereotactic radiation therapy provides benefit over conventional fractionated protocols due to reduced probability of cancer recurrence and increased comfort for the patient (Kranzinger et al., 2014, Polovnikov et al., 2013). Hypofractionated dosage protocols are commonly encountered in instances of medically inoperable head and neck cancer and/or as a boost therapy to malignancies previously treated with conventional external beam radiation therapy (Vargo et al., 2014; Yamazaki et al., 2014; Kress et al., 2014).

The causation of hearing loss due to stereotactic radiation therapy remains uncertain. Single dosages of > 13 Gy for vestibular schwannoma treatment have been associated with hearing loss and it has been suggested that cochlear dose is inversely related to hearing preservation (Yang et al., 2013; Hasegawa et al., 2013). The current study delivered dosages in the range appropriate for stereotactic radiation of vestibular schwannoma in an attempt to determine if cochlear damage could be identified shortly after cranial irradiation.

The effects of cranial irradiation upon the auditory system have been investigated using animal models, most often the guinea pig and rat. Tokimoto and Kanagawa (1985) examined the short-term effects of X-ray radiation upon hearing sensitivity in the Hartley guinea pig. Ultimately, they concluded that the degree of hearing loss in the initial 10 hours post-irradiation was dose-dependent while the onset of the hearing loss was inversely linked to irradiation dosage. Short-term post-irradiation ultrastructural changes were reported in the basal turn outer hair cells of the guinea pig within the initial 6 hours post-exposure to a single dose of 70 Gy (Winther, 1970). Inner hair cells and supporting cells throughout the cochlear length were unaffected by the irradiation, as were the apical hair cells (Winther, 1970). Similarly, in a study examining both short- and long-term effects of radiation dosages ranging from 1 – 30 Gy, Kelemen (1963) noted short-term damage only in the basal regions of the organ of Corti.

At this time, no studies have utilized a mouse to model short-term post-irradiation peripheral auditory effects. A mouse model would prove beneficial for a variety of reasons, including detailed knowledge of the genetic background, availability of genetically altered mice, and inclusion of molecular biology techniques to elucidate the mechanism of the hearing loss (Kikkawa et al., 2012). An additional benefit is the fact that the mouse is a viable model for the study of hearing impairment (Salvi and Boettcher, 2008; Ohlemiller, 2006; Friedman, Dror, and Avraham, 2007).

For the reasons listed above, this pilot study aims to investigate the mouse as an animal model for short-term post-irradiation hearing loss within the first post-exposure week. We

chose the 129Sv strain because it is bred in-house and we have an extensive normative database showing no age-related hearing loss at 9 weeks of age. We hypothesize that the mouse will serve as a viable model of study for short-term effects of cranial irradiation, including hearing loss and histopathological changes in the cochlea and auditory nerve.

Materials and Methods

Animals

129Sv mice of either sex, bred in-house were used (n = 27). The 129Sv mouse is often used in auditory research due to the presence of a normal allele preventing early-onset age-related hearing loss. The subjects were 9 weeks of age, approximating a young adult. Animals were included in the study only if baseline ABR thresholds (8, 16, 24, 32, and 40 kHz) were within +/− 10 dB SPL of the colony's ABR threshold averages. The animal care and use protocol was approved by the Institutional Animal Care and Use Committee (IACUC) of Saint Louis University School of Medicine, in accordance with Public Health Service (PHS) Policy in Humane Care and Use of Laboratory Animals, the U.S. National Institutes of Health (NIH) Guide for Care and Use of Laboratory Animals, and the U.S. Animal Welfare Act.

Experimental Design

The mice were randomly assigned to one of five groups: control (sham) (n = 3), 10 Gy (n = 4), 20 Gy (n = 4), 40 Gy (n = 4), and 60 Gy (n = 4). The Gy dosages selected for study were based upon Tokimoto and Kanagawa (1985) who reported no hearing loss at dosages < 40 Gy in guinea pigs. All mice had baseline hearing recorded within one week of scheduled irradiation. Mice meeting the inclusion criteria stated above were exposed to irradiation following which the ABR was repeated at four post-irradiation time points: 2, 4, 6, and 8 days. After the final ABR session, the mice were sacrificed and the cochlea were isolated and examined for structural alterations.

Auditory Brainstem Response (ABR)

Test subjects were sedated (Avertin [2,2,2-Tribromoethanol, Sigma Aldrich, St. Louis, MO] 0.4 mg/gm i.p.) and placed in a sound booth for testing. The mouse was positioned supine and the head rotated to direct the right ear superiorly and 6 cm directly below the speaker. Subdermal electrodes were placed at the vertex (noninverting), right pinna (inverting), and right rump (ground). Body temperature was maintained at 37°C using a thermoelectrical feedback system (FHC, Bowdoin, ME). Heart function was auditorily monitored. The ABR was measured at 5 frequencies (8, 16, 24, 32 and 40 kHz), using Tucker-Davis Technologies ABR Workstation. Tone-burst stimuli (20/sec) were presented in the sound field. Neural response waveforms (500) were collected over a 10 ms post-stimulus interval using a 20 kHz sampling rate. Threshold was defined as half the stimulus intensity interval (5 dB) between the lowest intensity producing a replicable response waveform and the intensity at which no response was elicited.

Irradiation

A calibrated XRAD320 Biological Irradiator™ with an adjustable podium from the radiation source was used. Calibration was performed using nanoDot dosimeters (Landauer, Inc.) placed at the irradiation position of a mouse head (see below for specific description of acrylic container). The resultant Gy levels were determined by Landauer, Inc. (3 nanoDots, each read in triplicate, per Gy dosage level). The deviation from intended Gy dosage (10, 20, 40, or 60 Gy) ranged from 0.04 – 2.80 Gy with larger deviations at the higher Gy levels. The sedated (Avertin, 0.4 mg/gm i.p.) mice were placed into an acrylic circular container (21.5 cm diameter, 7.5 cm height) divided into 8 pie-shaped compartments), with the heads positioned towards the cage center. A 5/8 inch lead shield in a “donut” configuration was placed on top of the mouse container to shield the mouse body from radiation, thus only exposing the head. The container holding the mice was positioned at a uniform height (mouse head at 40 cm) below the radiation source. A conversion table was used to determine the irradiation time needed to provide the total desired Gy dose. In determining irradiation time expressed as Gy level/minute, a formula based upon distance from the irradiator (40 cm) and irradiator settings of 320 kV and 12.5A was used (Gy dosage = 4.22 Gy/min). The total irradiation time was then calculated for each Gy dosage: 14.2 min for 60 Gy, 9.5 min for 40 Gy, 4.7 min for 20 Gy, and 2.4 min for 10 Gy.

Histological Preparation

Following the final ABR session at 8 days post-irradiation, mice in the 10, 20, and 60 Gy groups were prepared for structural analysis of the cochlea. The anesthetized mouse underwent transcardiac perfusion using 5 mL of phosphate-buffered saline followed by 10–20 mL of fixative (4% paraformaldehyde/2% glutaraldehyde in 0.1M cacodylate buffer). The cochleae were isolated, perilymphatically perfused, and immersed in fixative (OV, 4°C). The cochleae were postfixed in 1% osmium tetroxide and decalcified (120mM EDTA, 23°C, 24H). The cochleae underwent dehydration using a graded alcohol series following which the right cochlea was embedded in epoxy and cut in the mid-modiolar plane for examination by light and transmission electron microscopy (TEM) while the left cochlea was processed for scanning electron microscopy (SEM) analysis.

Morphometry

Spiral ganglion cells and their peripheral neural processes were quantified from mid-modiolar toluidine-blue thick sections. Five images of the lower basal and apical turns spaced 100 μm apart were digitally captured (40x) and archived from each cochlea (Nikon 80i, Retiga EXi, NIS-Elements, Melville, NY). The spiral ganglion cell count was conducted within a circular region (125 mm diameter). The criteria for a cell to be counted were: the presence of a nucleus, a clearly defined cell membrane, and at least half the cell inside the delineated circular area. The neuron count for peripheral processes in the spiral lamina was conducted within a region delineated by a trapezoidal template 160 mm in length, one height of 70 mm, and a second height of 37 mm. The criteria for a peripheral process to be counted included a discernable membrane and a longitudinal vs cross-sectional orientation.

Statistics

Statistical analysis was performed using SPSS (SPSS Software, Chicago, IL). Differences in threshold shift between experimental and control groups were evaluated using two-way ANOVA with factors of frequency and Gy group. Post-hoc analysis included the Dunnett t-test (2-sided) and Holm-Sidak test of multiple comparison. Since counts of spiral ganglion axons and cell bodies were virtually the same in the apical and basal turns, the data were combined into a single axon and single cell body entry for each cochlea/group. Differences in spiral ganglion (axons and cell bodies) density between experimental and control groups were evaluated using ANOVA, with post-hoc analysis using Holm-Sidak. Reliable differences were accepted with significance set at a p value ≤ 0.05.

Results

Auditory Brainstem Response

Table 1 lists the threshold shift and standard deviation for each combination of Gy group and post-irradiation testpoint. Overall, a larger variance was noted 8 days post-irradiation as compared to the earlier post-irradiation time points (Table 1). Although elevated thresholds were documented at all test frequencies in the 20 – 60 Gy groups, the elevation was usually most pronounced at 32 and 40 kHz.

In the 60 Gy group, the first significant threshold shift (mild, ~ 22 dB) was noted at all test frequencies at 6 days post-irradiation (Fig. 1A, cross) (ANOVA, $F_{(5, 80)} = 86.66$, p = 0.000). A progressive increase in threshold occurred from 6 to 8 days post-irradiation (Fig 1A) culminating in a moderate (~ 51 dB) degree hearing loss. A significant threshold shift at 32 kHz only was noted at 4 days post-irradiation in the 40 Gy group (Fig. 1B, square) (ANOVA, $F_{(6, 95)} = 167.86$, p = 0.000). By 8 days post-irradiation (Fig. 1B, triangle), a mild (~ 23 dB) elevation in threshold was noted at all test frequencies. In contrast, a significant threshold shift at 40 kHz was not noted until 6 days post-irradiation (Fig. 1C, cross) in the 20 Gy group (ANOVA, $F_{(5, 80)} = 86.66$, p = 0.000). The threshold elevation progressed to a mild (~ 19 dB) degree at all test frequencies by 8 days post-irradiation (Fig. 1C, triangle). Post-hoc analysis did not reveal significant threshold shift at any post-irradiation time point for the 10 Gy group (Dunnett t test, p > 0.050) (Fig. 1D).

Animal Health: Weight, Feeding, and Hydration

No changes in overall animal health were noted in the 10 Gy group. However, there was a consistent trend of weight loss beginning at 4 days post-irradiation with a loss of 10% body weight for mice in the 20 – 60 Gy groups. By 8 days post-irradiation, the mouse had lost up to 30% of total body weight. These weight changes were uncorrelated to the increasing Gy level exposure. The mice were not ingesting the same amount of water or food as their non-irradiated littermates. Avoidance behaviors such as turning the head aside or pushing the feeding tube away were noted when attempts were made to hand-feed the mice with a mix of water and Vetoquinol (Quebec, Canada), a high calorie oral nutritional supplement. Damage to the mucosal tissue lining the pharynx following the cranial irradiation most likely made swallowing painful, resulting in the observed feeding and drinking avoidance behaviors.

Ultrastructural Analysis

Intact stereocilia bundles and a cuticular plate are observed by SEM for the single row of inner hair cells and three rows of outer hair cells throughout the cochlear length at 8 days post-irradiation with 60 Gy (Fig 2). The ultrastructural analysis was extended to the cross-sectional view of the organ of Corti using TEM and high power light microscopy of toluidine-blue stained thick sections. Both the inner and outer hair cells appeared normal with the occasional appearance of a vacuole (Fig. 4B). Figure 3A shows the apical and basal stria vascularis displaying normal cytoarchitecture at 8 days post-irradiation with 60 Gy. At higher magnification, no detectable damage was noted to the capillary endothelial cells (Fig. 3B).

In contrast to the normal appearing organ of Corti and stria vascularis, pathology was noted in the apical and basal spiral ganglion cell peripheral processes in the 60 Gy irradiated cochleae. Extracellular matrix material between the 8^{th} n. neurons in the spiral lamina (Fig. 4B, arrows) was sparse or electron lucent. The density of the apical and basal neurons (Table 2) was also decreased in comparison to the lower Gy groups (ANOVA, $F_{(2,17)} = 8.023$, $p = 0.044$; post-hoc analysis: Holm-Sidak, $p < 0.05$).

The loss of extracellular matrix material was also observed among the spiral ganglion cells in Rosenthal's canal (Fig. 5B) of cochleae exposed to 60 Gy. Additionally, the remaining spiral ganglion and satellite cells showed evidence of vacuoles with some cells undergoing cell death. The size of viable spiral ganglion cells is equivalent to that of the control mouse (Fig. 5A). However, the density of the seemingly viable spiral ganglion cells in the 60 Gy group was significantly lower than cell density in the 20 Gy, 10 Gy or control mice (ANOVA, $F_{(2,17)} = 13.762$, $p < 0.001$; post-hoc analysis: Holm-Sidak, $p < 0.05$). As evident in comparing Rosenthal's canal of a control mouse (Fig. 5A) and that of a 60 Gy group mouse at 8 days post-irradiation (Fig. 5B), the loss of cells appeared to be more at the periphery of Rosenthal's canal with the more densely packed central region less affected.

Although the spiral ganglion cell density in the 20 Gy group was equivalent to that of the 10 Gy and control cochleae, the 20 Gy mice did have a mild high frequency loss at and above 24 kHz. High power examination of the spiral ganglion region showed evidence of cellular distress with vacuoles present in some cells, usually satellite cells (Fig. 5C). These cells seemed to be located closer to the periphery of Rosenthal's canal. Finally, as depicted in Fig. 5D, retraction of the satellite cell cytoplasm resulted in a separation of the spiral ganglion cell from its satellite cell.

Discussion

Overall, there was a significant threshold shift noted in mice exposed to a single dose ≥ 20 Gy. No short-term threshold shift occurred in the first week for mice exposed to 10 Gy irradiation, thus the threshold for hearing loss after single dose irradiation lies between 10 – 20 Gy. With one exception, (32 kHz, 4 days post-irradiation, 40 Gy), onset of a high frequency hearing loss occurred 6 days post-irradiation. The hearing loss progressed in severity and range, and all test frequencies were affected by 8 days post-irradiation. Histopathological examination at 8 days post-irradiation revealed a dramatically decreased

density in spiral ganglion cell bodies and their peripheral processes, as well as a loss of the associated extracellular matrix in mice exposed to 60 Gy. Negligible changes were seen in the outer and inner hair cells, with overall preservation of the stria vascularis and cochlear vasculature.

Tokimoto and Kanagawa (1985) found that onset of hearing loss was inversely linked to irradiation dosage (20 – 80 Gy) in Hartley guinea pigs with initial onset 3 – 10 hours post-irradiation. Conversely, our study in mice found onset of hearing loss (6 days post-irradiation) was constant for 20 –60 Gy exposures. However, threshold shift progressed by 8 days post-irradiation to a mild hearing loss in 20 and 40 Gy mice, but a moderate loss in the 60 Gy mice, indicating some interaction between dosage and threshold shift.

Winther (1970) used an opening in a lead shield to focus approximately 70 Gy to the left half of the guinea pig skull. This focused exposure resulted in nuclear, then cytoplasmic changes in basal outer hair cells as quickly as 3 and 4 hours post-irradiation, respectively. At 6 hours post-irradiation, debris from degenerating outer hair cells in the basal cochlear turns was noted. Winther reported the apical outer hair cells and all inner hair cells appeared normal, a finding reproduced by the Tokimoto and Kanagawa in guinea pigs with radiation doses ranging from 20 – 120 Gy (1985). Using a mouse model from the 129Sv strain, our study did not replicate such histologic changes in the basal outer hair cells. This may be due to the higher Gy level (Wither, 1970; Tokimoto & Kanagawa, 1985), the more focused irradiation beam (Winther, 1970), and/or an interspecies variance in the cochlear response (i.e. guinea pigs vs mice). Interestingly, via SEM, Tokimoto and Kanagawa (1985) showed that the cuticular plate and stereocilia of both inner and outer hair cells appeared normal (10 Gy, 6 hours post-irradiation), a finding replicated in our study.

Atlas et al. (2006) noted degeneration of the stria vascularis and spiral ligament as early as 4 hours post-irradiation (fractionated dose equivalent to 60 Gy) in the guinea pig. In the current study, the stria vascularis appeared normal with no devascularization or endothelial cell injury noted 8 days post-irradiation. Likewise, Winther (1970) found no discernible cochlear devascularization in the guinea pig. The lack of vascular change noted in the present and Winther (1970) studies does not support devascularization as an etiology for radiation-induced threshold elevation as has been proposed by Wackym et al (2010).

Using fractionated irradiation equal to 60 Gy, Atlas et al. (2006) reported decreased spiral ganglion cell density at 4 hours (66%), 24 (80%), and 96 hours (88%) post-irradiation in a guinea pig. The decrease in spiral ganglion nerve cell bodies and peripheral processes in the 60 Gy mice of the current study was far less pervasive. More interestingly, in the 20 Gy group, which incurred only a mild threshold shift, vacuolization and separation of the spiral ganglion cell from its supporting satellite cell and early signs of possible demyeliniation were noted. Similar findings are reported 1 day post-noise exposure in the CBA mouse (Wang et al., 2002). Likewise, Tagoe et al. observed demyelination 4 – 5 days post-acoustic overstimulation in young rats (2014). Demyelination by doxorubicin injection into the 8th n. was also found by El-Badry et al. (2007). Xing et al. (2012) noted similar histopathology in aged CBA mice and noted that demyelination correlated to a decline in the expression level of MBP (2012). The combination of these reports and our findings add to the growing body

of evidence that demyelination is an early sign of cochlear pathology and can affect auditory function. Further study regarding this possible mechanism of post-irradiation effects is warranted.

Our study is the first to use a mouse model to examine short-term, post-cranial irradiation peripheral auditory effects. The animal irradiator used in this study did not have the capability to focus radiation to a small, well-defined area of the skull as does the microRT (Kiehl et al., 2008). Despite the use of lead body shielding, the entire head and neck vs only the cochleae were exposed to irradiation with the result that mice receiving > 10 Gy experienced a loss of up to 30% of total body weight by 8 days post irradiation. This side effect was the same in severity across the 20 – 60 Gy groups and is unrelated to the peripheral auditory changes.

Current treatment protocols for radiation treatment of vestibular schwannoma commonly include stereotactic radiosurgery and hypofractionated/conventionally fractionated stereotactic radiation therapy. Based upon the results of this pilot study in which the threshold for short-term hearing loss was > 10 Gy but < 20 Gy, we recommend a fractionated irradiation dosage of 10 Gy for investigations using the mouse model. This dose best simulates that received by the cochlea in therapeutic cranial irradiation (Hasegawa et al., 2011; Yang et al., 2010). Future studies could extend the post-exposure time to 3 weeks and/or 12 weeks to investigate whether later developing short-term effects, as observed in patients receiving cranial irradiation, occur in the mouse model. Implementation of the 10 Gy protocol using the mouse as a model would allow the investigator to have increased knowledge of genetic background and with access to genetically altered mice, permit inclusion of molecular biology techniques for mechanistic study of the short-term hearing loss (Kikkawa et al., 2012). Ultimately, it is our hope that the results of this pilot study can prompt further research to elucidate underlying mechanisms of irradiation-induced hearing loss and optimize therapeutic irradiation regimens, resulting in more satisfactory hearing sensitivity outcomes in patients receiving cranial irradiation for various head and neck malignancies.

Acknowledgements

Transmission electron microscopy was conducted at the Microscopy and Digital Imaging Core of the Research Center for Auditory and Vestibular Studies at Washington University (NIH-NIDCD P30 DC004665). The technical assistance of Grady Philips, M.S. is gratefully appreciated. The authors wish to thank Richard Di Paolo, Ph.D. and his lab for access to the XRAD320 Biological Irradiator™ and sharing of their technical knowledge. The authors also extend their thanks to Landauer, Inc. for their donation of nanoDots and assistance in calibration. Finally, the authors wish to thank the Office of Radiation Safety at Saint Louis University for their time and assistance in the calibration procedures.

Supported in part by DC006422 from the NIDCD to MAG and the Saint Louis University School of Medicine Otolaryngology Resident Research Fund

References

1. Bhandare MS, Jackson A, Eisbruch A, et al. Radiation Therapy and Hearing Loss. Int J Radiat Oncol Biol Phys. 2010; 76:S50–S56. [PubMed: 20171518]

2. Kranzinger M, et al. Hypofractionated stereotactic radiotherapy of acoustic neuroma: Volume changes and hearing results after 89-month median follow-up. Strahlenther Onkol. 2014; 190(9): 798–805. [PubMed: 24638268]
3. Polovnikov ES, et al. Stereotactic radiosurgery and hypofractionated stereotactic radiotherapy for management of vestibular schwannomas: Initial experience with 17 cases. Acta Neurochir Suppl. 2013; 116:37–44. [PubMed: 23417456]
4. Vargo JA, Ferris RL, Clump DA, Heron DE. Stereotactic body radiotherapy as primary treatment for patients with medically inoperable head and neck cancer. Front. Oncol. 2014; 4(214):1–6. [PubMed: 24478982]
5. Yamazki H, et al. Hypofractionated stereotactic radiotherapy using CyberKnife as a boost treatment for head and neck cancer, a multi-institutional survey: Impact of planning target volume. Anticancer Res. 2014; 34:5755–5760. [PubMed: 25275085]
6. Kress MAS, et al. Safety and efficacy of hypofractionated stereotactic body irradiation in head and neck cancer: Long-term follow-up in large series. Head. Neck. 2014
7. Yang I, Sughrue ME, Han SJ, Aranda D, Pitts LH, Cheung SW, Parsa AT. A comprehensive analysis of hearing preservation after radiosurgery for vestibular schwannoma: Clinical Article. J Neurosurg. 2013; 119(Suppl):851–859. [PubMed: 25077322]
8. Hasegawa T, Kida Y, Kato T, Iizuka H, Yamamoto T. Factors associated with hearing preservation after Gamma Knife surgery for vestibular schwannomas in patients who retain serviceable hearing. J Neurosurg. 2011; 115(6):1078–1086. [PubMed: 21961962]
9. Tokimoto T, Kanagawa K. Effects of X-ray Irradiation on Hearing in Guinea Pigs. Acta Otolaryngol. 1985; 100:266–272. [PubMed: 4061077]
10. Winther FO. X-ray irradiation of the inner ear of the guinea pig-An electron microscopic study of the degenerating outer hair cells of the Organ of Corti. Acta Otolaryngol. 1970; 69:61–76. [PubMed: 5446609]
11. Kelemen G. Radiation and Ear. Experimental Studies. Acta Otolaryngol. 1963; 184(Suppl 184):1–48.
12. Kikkawa Y, et al. Advantages of a Mouse Model for Human Hearing Impairment. J Exp Anim Sci. 2012; 61:85–98.
13. Salvi, R.; Boettcher, F. Sourcebook Models for Biomedical Research. Totowa: Humana Press; 2008. Animal Models of Noise-Induced Hearing Loss.
14. Ohlemiller KK. Contributions of mouse models to understanding of age- and noise-related hearing loss. Brain Res. 2006; 1091:89–102. [PubMed: 16631134]
15. Friedman LM, Dror AA, Avraham KA. Mouse models to study inner ear development and hereditary hearing loss. Int J Devel Bio. 2007; 51:609–631. [PubMed: 17891721]
16. Atlas E, Ertekin MV, Gundogdu C, Demirci E. L-Carnitine Reduces Cochlear Damage Induced by Gamma Irradiation in Guines Pigs. Ann Clin Lab Sci. 2006; 36(3):312–318. [PubMed: 16951273]
17. Wackym PA, Runge-Samuelson CL, Nash JJ, Poetker DM, Albano K, Bovi J, Michel MA, Friedland DR, Zhu Y, Hannley MT. Gamma Knife Surgery of Vestibular Schwannomas: Volumetric Dosimetry Correlations to Hearing Loss Suggest Stria Vascularis Devascularization as the Mechanism of Early Hearing Loss. Otol Neurotol. 2010; 31:1480–1487. [PubMed: 20930653]
18. Wang Y, Hirose K, Liberman MC. Dynamics of noise-induced cellular injury and repair in the mouse cochlea. J Assoc Res Otolaryngol. 2002; 3:248–268. [PubMed: 12382101]
19. Tagoe T, Barker M, Jones A, Allcock N, Hamann M. Auditory nerve perinodal dysmyelination in noise-induced hearing loss. J Neurosci. 2014; 34:2684–2688. [PubMed: 24523557]
20. El-Badry MM, Ding DL, McFadden SL, Eddins AC. Physiological effects of auditory nerve myelinopathy in chinchillas. Eur J Neurosci. 2007; 25:1437–1446. [PubMed: 17425569]
21. Xing Y, Samuvel DJ, Stevens SM, Dubno JR, Schulte BA, Lang H. Age-related changes of myelin basic protein in mouse and human auditory nerve. PLoS One. 2012:7e34500.
22. Kiehl EL, et al. Feasibility of small animal cranial irradiation with the microRT system. Med Phys. 2008; 36:4735–4743. [PubMed: 18975718]

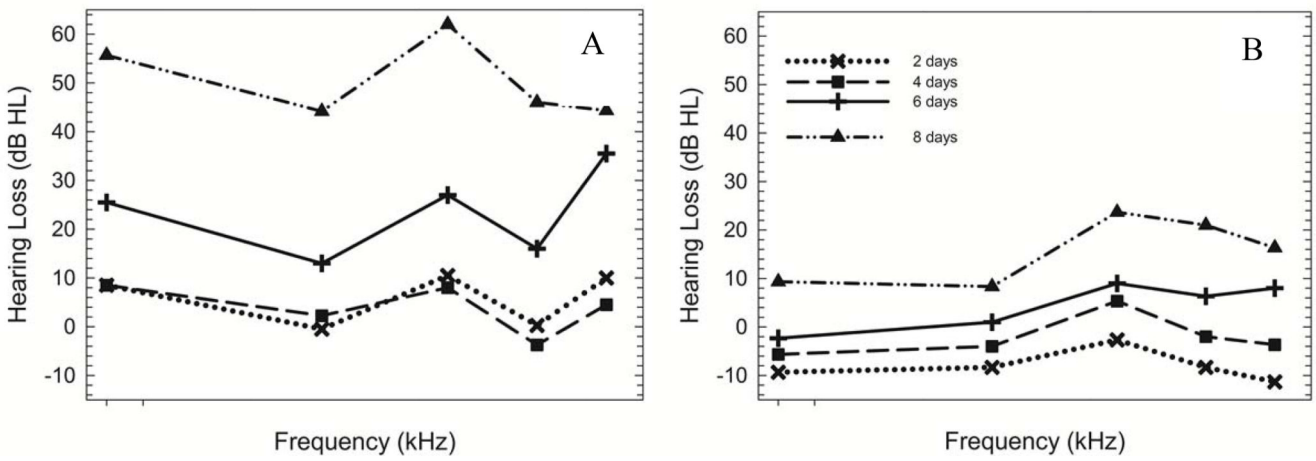

Figure 1. ABR threshold shift as a function of post-irradiation time

Mean ABR threshold shifts plotted at 2 days (x), 4 days (square), 6 days (cross), and 8 days (triangle) post-irradiation in 60 Gy (**A**), 40 Gy (**B**), 20 Gy (**C**), and 10 Gy (**D**) groups. For variance, see Table 1. Overall, there was a significant threshold shift noted in mice exposed to 20 Gy, 40 Gy, and 60 Gy. The hearing loss was progressive beginning in the high frequencies at 4 days post-irradiation in the 40 and 60 Gy groups but not until 6 days post-irradiation in the 20 Gy group. The degree of hearing loss was dependent upon the Gy level exposure. No significant threshold shift occurred in mice exposed to 10 Gy.

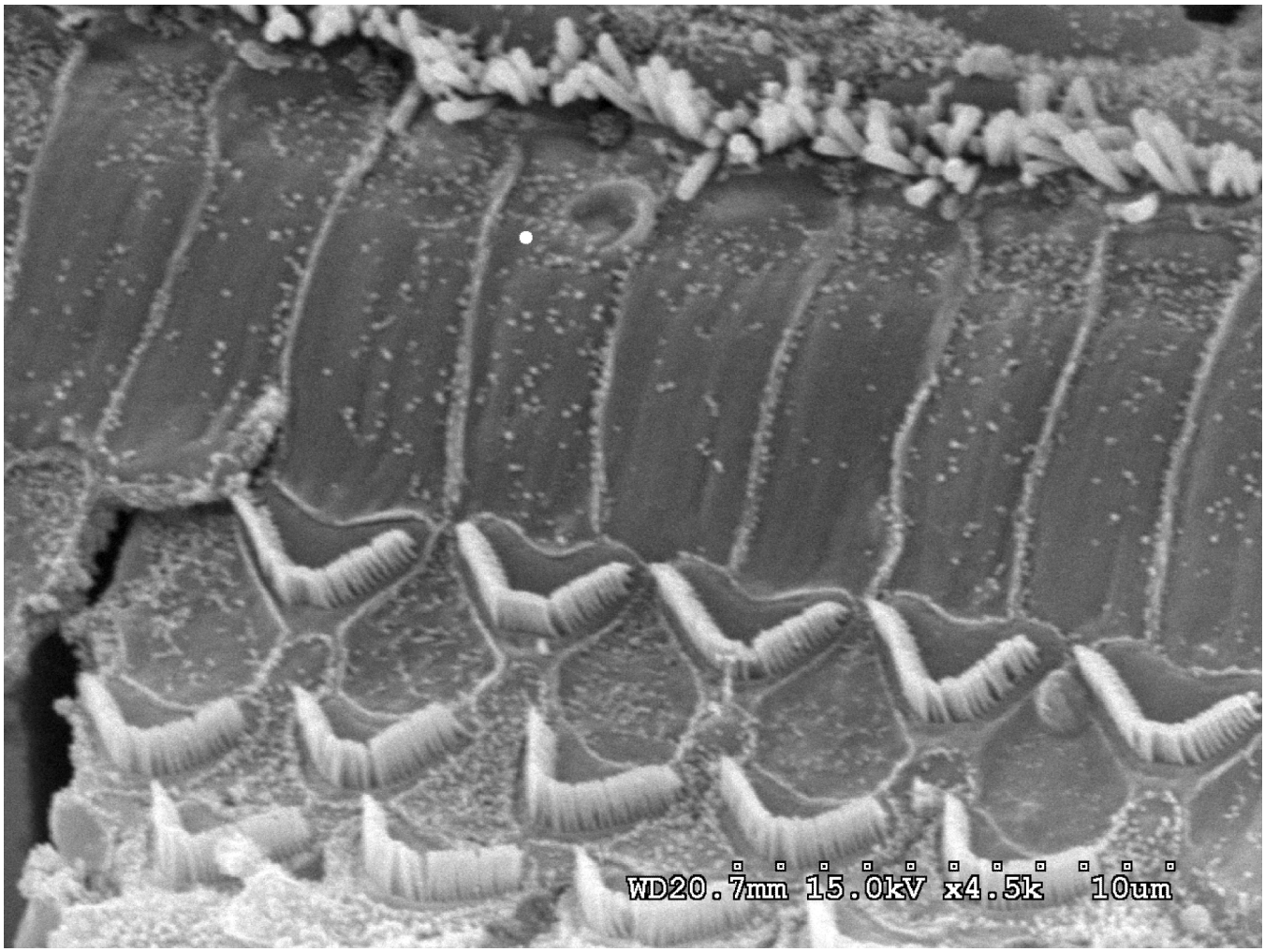

Figure 2. Organ of Corti is grossly unaffected by irradiation in the 60 Gy group

Basal turn SEM shows that inner hair cells (IHCs) and outer hair cells (OHCs) appeared structurally intact without any evidence of damage or deterioration at 8 days post-irradiation. Scale bar = 10 μm

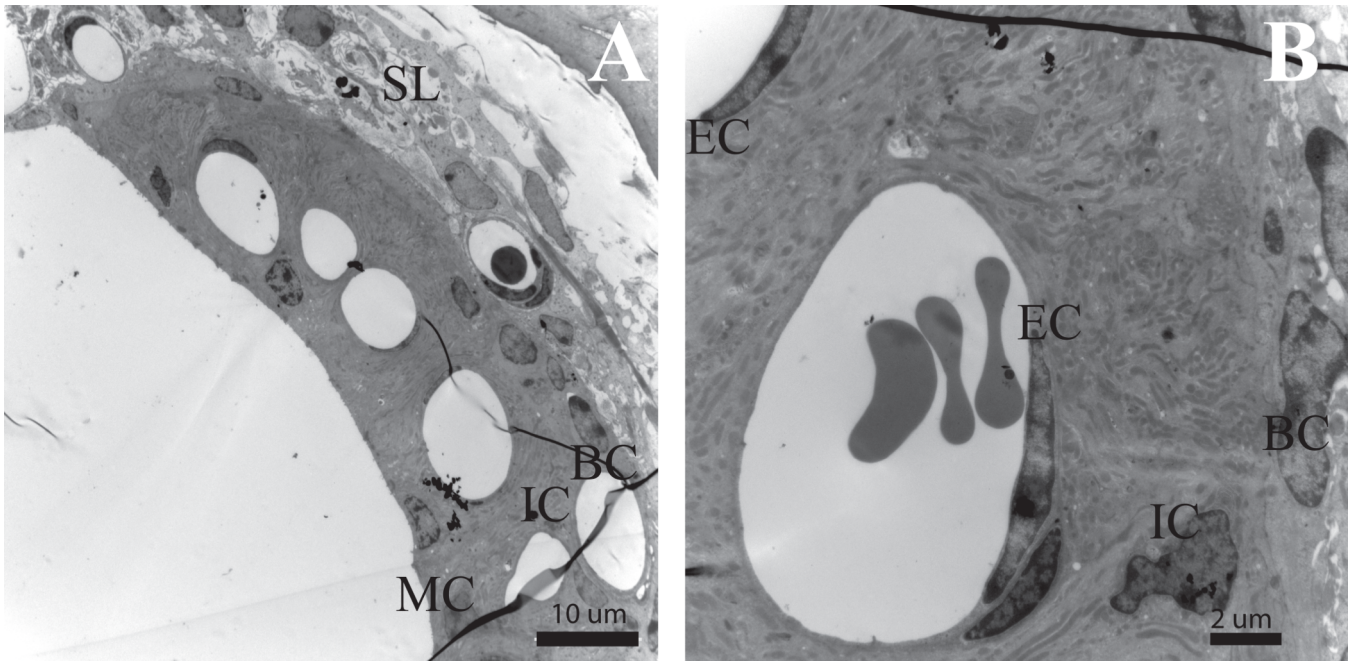

Figure 3. Stria vascularis (SV) shows no radiation-induced changes in the 60 Gy group

(**A**) Tissue of the cochlear lateral wall shows no evidence of edema, vacuoles or nuclear condensation in either the fibrocytes of the spiral ligament or the three cell layers of the stria vascularis. Normal capillary density is evident in this mid-modiolar cross-section of the 60 Gy SV at 8 days post-irradiation. **(B)** Normal capillary wall endothelium and surrounding SV in a control mouse. (C) Normal capillary wall endothelium and surrounding SV in 60 Gy mouse at 8 days post-irradiation. SL = Spiral Ligament, BC =Basal Cell, IC =Intermediate Cell, MC =Marginal Cell, EC = Endothelial Cell, PC= Pericyte, Cap=Capillary Scale bar A=10 μm, B=2 μm

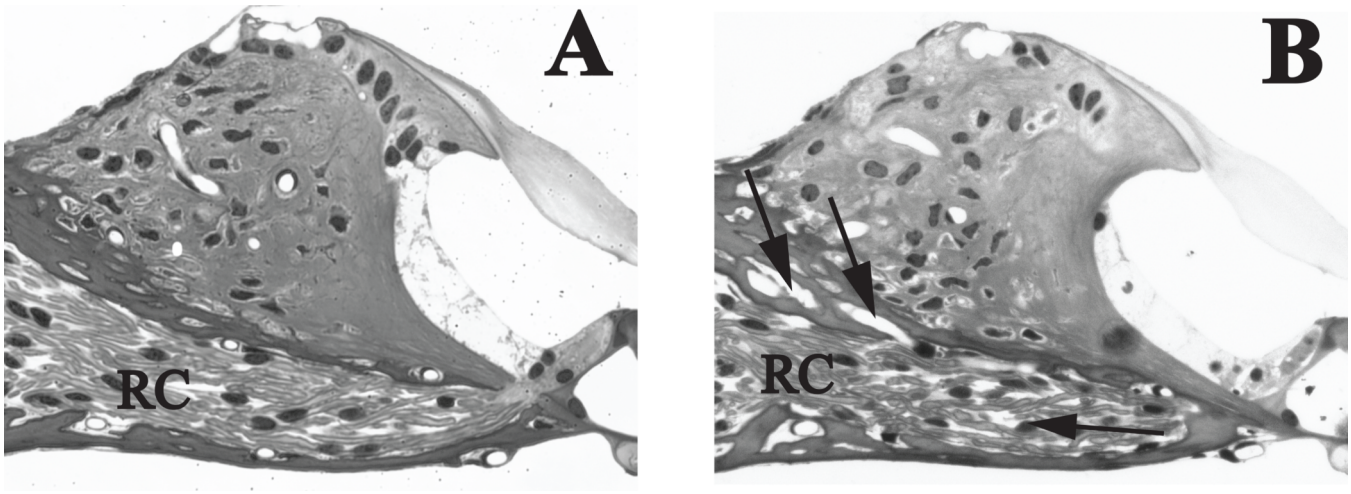

Figure 4. Axonal density traversing spiral lamina is decreased in the 60 Gy group

(A) The auditory nerve fibers in the spiral lamina of a control mouse show minimal area unoccupied by bipolar axons or extracellular matrix. **(B)** The spiral lamina of a mouse 8 days post-irradiation with 60 Gy has areas devoid of axons, glia or extracellular matrix (arrows) at 8 days post-irradiation. Although the cells of the organ of Corti from spiral limbus to inner pillar cell appear normal, a vacuole (arrowhead) can be detected at the base of the inner hair cell. AN= auditory nerve fibers, SpL= spiral limbus, tm= tectorial membrane. Scale bar= 50 μm

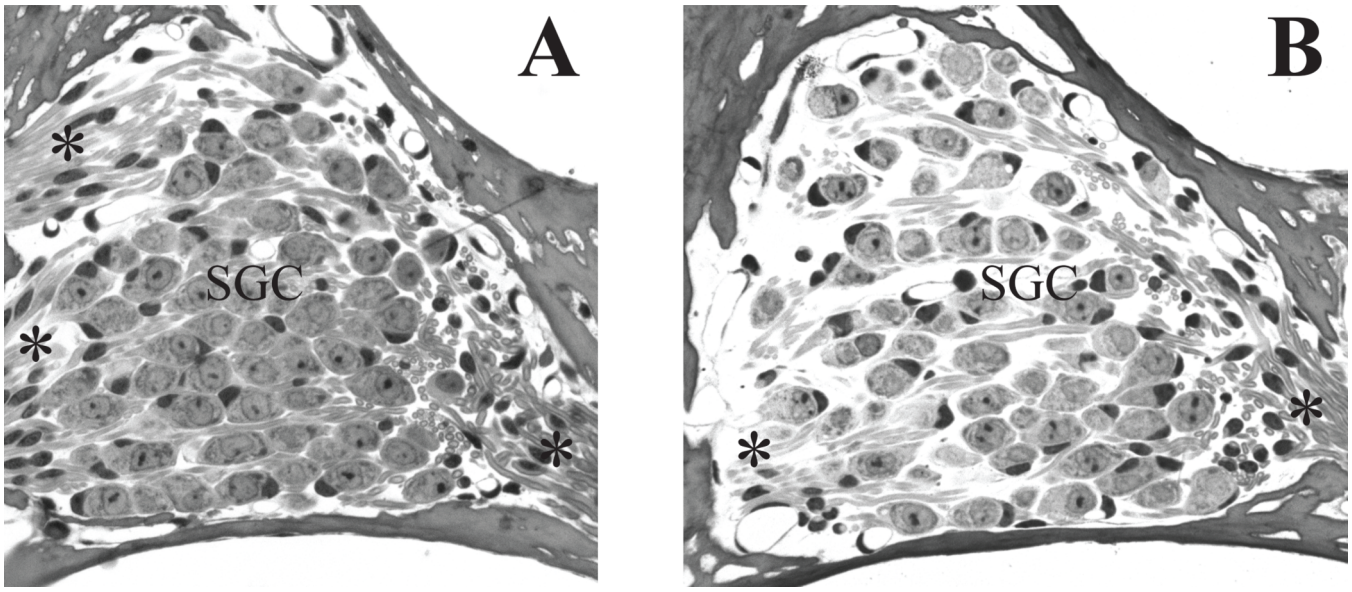

Figure 5. Spiral ganglion (SG) cell density is decreased in the 60 Gy group

(A) Rosenthal's canal in a control mouse shows a high density of spiral ganglion cells and associated axon bundles. **(B)** Decreased SG and extracellular matrix density is evident in the 60 Gy group at 8 days post-irradiation (arrows). Vacuoles are present in some of the remaining SG/satellite cell complexes (arrowheads). **(C)** An early marker of irradiation-induced cellular stress is vacuolization (arrowheads) in the satellite cells of a mouse at 8 days post-irradiation with 20 Gy. **(D)**. Satellite cells (white dot on nucleus) show reduced cytoplasm and retraction (arrowheads) from their adjacent spiral ganglion cell. SGC=spiral ganglion cells, *= peripherally directed axons; **= centrally directed axons. Scale bar A&B= 20 μm, C&D = 5 μm

Table 1

ABR mean threshold shift and standard deviation as a function of Gy group

		8 kHz		16 kHz		24 kHz		32 kHz		40 kHz	
		X	SD	X	SD	X	SD	X	SD	X	SD
60 Gy	**2d**	4.4	4.1	4.3	2.5	6.3	4.1	5.1	7.1	7.5	4.1
	4d	4.4	4.1	7.0	8.2	3.8	5.0	1.1	4.1	2.0	5.0
	6d	21.4	4.1	17.8	4.8	22.8	2.9	16.9	4.8	33.0	9.6
	8d	52.4	13.0	50.2	16.6	58.7	15.9	52.1	13.0	43.5	4.3
40 Gy	**2d**	7.4	4.1	2.5	5.0	3.3	4.1	2.6	2.9	2.5	0.0
	4d	6.9	6.5	6.8	2.5	8.8	5.0	17.1	7.1	10.8	4.8
	6d	11.7	6.3	5.8	8.5	9.8	5.0	14.9	4.8	16.0	2.9
	8d	23.0	10.8	27.8	14.4	22.0	8.7	15.3	12.6	24.7	2.9
20 Gy	**2d**	−1.2	2.9	−3.7	2.9	−6.3	2.9	−9.5	2.9	−6.8	2.9
	4d	2.4	10.0	0.7	2.9	1.7	2.9	−3.2	5.8	0.8	2.9
	6d	5.8	2.9	5.7	2.9	5.3	5.0	5.1	0.0	12.5	0.0
	8d	17.4	13.2	13.0	13.2	20.0	20.8	19.5	18.9	24.2	16.1
10 Gy	**2d**	10.4	5.0	6.0	5.0	1.7	5.8	−0.9	8.7	3.2	2.9
	4d	3.4	5.0	4.3	2.9	5.0	2.9	5.5	2.9	6.2	2.9
	6d	2.1	2.9	1.3	2.9	5.0	2.9	−2.2	2.9	7.8	2.9
	8d	2.8	2.9	−3.3	2.9	4.3	5.0	2.5	7.6	2.5	5.0

Table 2

Mean Cell Counts/Gy Group

	Spiral lamina neurons	SD	Spiral ganglion cells	SD
60 Gy	40.2	5.2	33.0	3.8
20 Gy	50.6	0.8	39.9	2.1
10 Gy	49.6	2.9	40.1	1.9
Control	54.1	8.7	40.1	1.8